RIVA: a new experimental facility for fast blowdown and pressurization of small containment

Lucia Sargentini, Constantin Ledier, Arnaud Chazottes

RIVA: A NEW EXPERIMENTAL FACILITY FOR FAST BLOWDOWN AND PRESSURIZATION OF SMALL CONTAINMENT

Lucia Sargentini, Constantin Ledier and Arnaud Chazottes
Université Paris-Saclay, CEA, Service de Thermohydraulique et de Mécanique des Fluides,
91191, Gif-sur-Yvette, France
lucia.sargentini@cea.fr; constantin.ledier@cea.fr; arnaud.chazottes@cea.fr

[leave space for DOI, which will be inserted by ANS]

ABSTRACT

In case of Main Steam Line Break scenarios, several thermal hydraulics phenomena, such as two-phase critical flow, wall condensation, and stratification of the atmosphere of the containment are involved. The RIVA facility is devoted to the study of such phenomena by means of a fast blowdown of a vessel discharging in a containment. A valve near the inlet of the containment vessel with a fast opening actuator is used to simulate the sudden break of the secondary loop of a nuclear reactor. The entire device is highly instrumented, especially the containment with more than 200 thermocouples. Moreover, two instrumentation sections on the connection pipe allows us to measure local pressure, pressure drop and local temperature before the inlet of the vessel. At first, some experiments are realized by replacing steam by nitrogen, to understand the behavior of the fluid during a very fast blowdown, changing the outlet section of the line. These experiments indicate that a chocked flow is present and allow us to study the influence of temperature, mass flow rate and pressure at the injection section on the jet plume in the vessel. Subsequently, experimental tests with steam and then with some structures in the containment vessel have been realized. They have allowed a better understanding of the wall condensation phenomenon and the effects of the volume occupation rate. The analyses of the results are not presented in the document but will in coming articles.
In the same way, further experiments with a steam blowdown have been performed to take into account the wall condensation and will be the subject of a future article.

KEYWORDS
Fast blowdown, critical flow, experiments, fast pressurization, small containment

1. INTRODUCTION

The containment of a nuclear power plant is the last safety barrier to avoid the release of radioactivity in the environment [1]. It is therefore essential to assure its integrity during any accident. In particular, during a Main Steam Line Break (MSLB) [2], the secondary circuit is broken and a blowdown begins. The fluid (water vapor at the beginning and two-phase flow later) flows toward the containment through the break. This causes the pressurization of the containment and the increase of its temperature. This situation could lead to reach the maximum pressure and temperature acceptable in the containment. To evaluate these two variables, codes for simulating the behavior of the containment are developed (e.g. [3]–[7]). To assess and validate these codes and to understand the physical phenomena relevant for the drop of the pressure and temperature in the containment, over the years a quite large number of test facilities (e.g. MISTRA [8], TOSQAN [9], PANDA[10], THAI [11]) were used. These facilities are dedicated to the study of the thermal stratification, hydrogen distribution, wall condensation and the behavior of air/steam/hydrogen mixture. More recently, ATLAS/CUBE [12] facility was designed to couple the Integral Effect Test facility ATLAS with a containment simulator (CUBE). It aims at analyzing the interaction between the reactor system and

the containment for a PWR during a Small Break LOCA. For example, it is possible to evaluate the mass/energy in the containment from the measured two-phase critical flow at break nozzle.
Every facility cited above is scaled for representing a large reactor containment, such as Pressurized or Boiling Water Reactor (PWR or BWR) containment. The increasing interest in the nuclear community for the concept of compact reactors leads to the need in the analysis of small containments. Actually, during a postulated MSLB occurring with the same quantity of steam at the break, small containments can reach higher peak of pressure and higher peak of local temperature with respect of large containments due to the reduced dimensions and the space requirements. These peaks are the fundamental quantities for the design and the safety assessment of the new concepts of small reactor containments.
Fang et al. [13] focuses on the analysis of an upward steam jet in a complex small structure. The device is composed by a steel building with compartments representing the several components of a small nuclear power plant. Fang et al. focuses on the temperature of the jet and the temperature field in the containment. Unfortunately, pressure is not analyzed. Moreover, the steam is not pressurized and the velocity of the jet is quite modest. These conditions are not representative of a MLSB for small PWR reactors. Recently, the Core Make Up Tank (CMT) is built at State Power Investment Corporation (SPIC) Research Institute in China [14] to analyze the blowdown in the CMT tank of the Westinghouse AP-series PWRs. Even if the goal of this facility is not to produce data for the containment analysis, it can address some interesting phenomena, as the wall heat exchange. In this context, to improve the knowledge of small containment behavior, the RIVA facility has been built. The goal of this facility is to reproduce a fast blowdown of a steam generator and a consequently fast pressurization of a small containment vessel.

The article presents the experimental facility RIVA and the first experiments conducted with nitrogen. It is organized as follows. In Section 2, the RIVA facility is described. In Section 3, the analysis of a nitrogen fast blowdown is presented. Then, the comparison between the experiment and the system code CATHARE2 is detailed in Section 4. At the end, conclusions are drawn.

2. PRESENTATION OF THE EXPERIMENTAL FACILITY RIVA

The RIVA experimental set-up (Figure 1) is composed of:

- a steam generator of about 1m^3 and thermally insulated;
- a containment of roughly some tens of m^3;
- a connection line of about 50 mm nominal diameter and 10 m long.

A detailed description of the facility and of its instrumentation is presented in the following part.

2.1. Description of the test facility RIVA

The steam generator is a pressurized vessel, which contains a heater to heat the fluid at the beginning of every experience. The connection line is the pipe connecting the steam generator and the containment. It is composed by several components. The first one is the isolation valve located at the top of the steam generator. It ensures its isolation from the rest of the installation during the heating phase. Further, the mass flow meter section consists in a divergent section, a bigger diameter section (DN200) and a convergent section. In the bigger section, there is a mass flow meter.
An instrumented section is located upstream of the containment. It allows measuring the pressure and temperature of the steam as close as possible of the entrance of the containment.
The fast opening valve is installed between the containment and the instrumentation section. Its fast opening allows a brutal discharge of the steam generated in the steam generator towards the containment.
To study different flow configurations, different injection nozzles were installed at the end of the connection line at the top of the containment. Moreover, an injection system called "jet-breaker" can be used. It is composed by the injection tube with a blind flange obstructing the outlet. Thus, the fluid collides the flange and directs radially instead of flowing down in the axial direction.

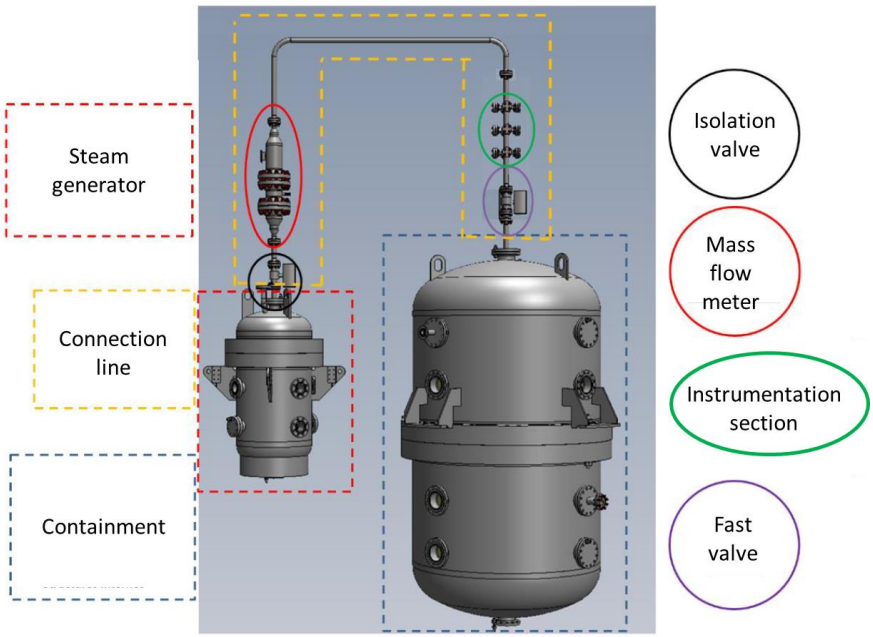

Figure 1: Sketch of RIVA facility

2.2. Instrumentation of the RIVA facility

In the steam generator, pressure measurements, vertical distribution of the gas temperatures and internal and external wall temperatures are available (Figure 2).

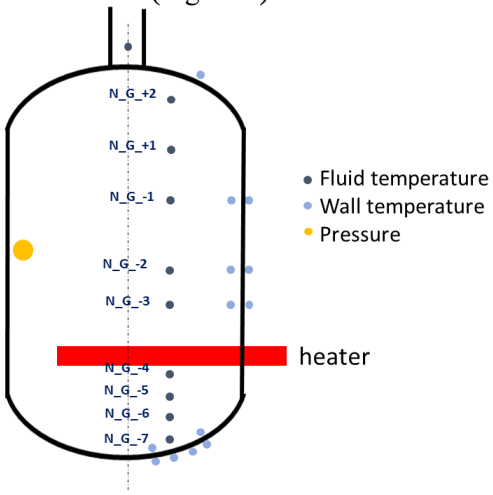

Figure 2: Sketch of RIVA instrumentation for the steam generator

The connection line is a well-instrumented part of the installation (Figure 3). It contains:

- several thermocouples for the external wall temperatures to regulate the heat blankets;
- a mass flow meter positioned in the flowmeter section. Measurement is carried out using a primary element for which the local pressure loss coefficient is known. Moreover, the absolute pressure (CP7_Qm) and fluid temperature (T_G_Qm) is measured at the same location;
- two differential pressure sensors are installed between the inlet and outlet of the instrumentation section (DP);
- an absolute pressure sensor (CP5_T_P+1) is located at the outlet of the instrumentation section;

- two gas thermocouples (TG_P_P+3 and TG_P_P+1) are available respectively at the inlet and outlet of the instrumentation section.

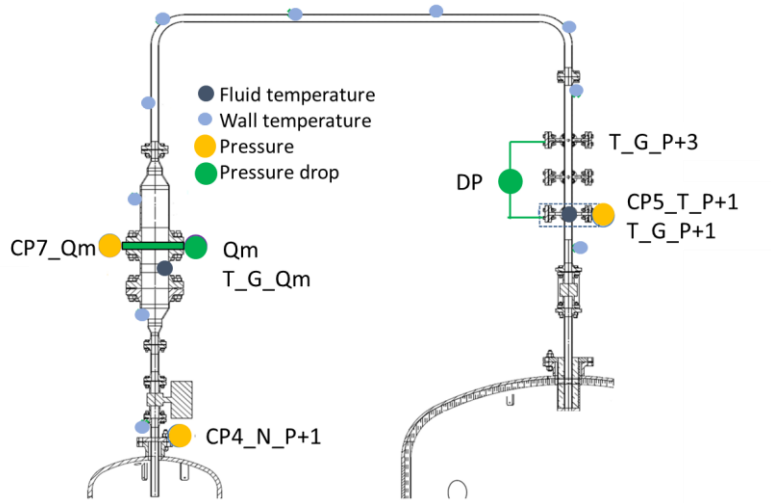

Figure 3: Sketch of RIVA instrumentation for the connection line

A large number of sensors are available in the containment (about 150):

- for the fluid temperature, several thermocouples are supported by a stainless steel structure and distributed in the whole containment. They allow presenting a quite fine spatial resolution of the temperature. Thermocouples are disposed at different height and two different angles. In particular, thermocouples are arranged on 12 levels (from C+6 to C-6) and 5 radii (from R1 at the axis to R5 close to the wall) on the 45° vertical plane and only 6 levels and 3 radii on the 135° vertical plane;
- a second set of thermocouples, positioned on the whole height of the shell and the caps of the receiver, allows to measure the temperature on the internal and external faces of the receiver;
- three pressure sensors are also available: two absolute pressure sensors positioned respectively in the upper and lower parts of the containment (CP3_R_P+1 and CP2_R_P-1) and a relative pressure sensor (CP1_R_P-1) in the same position as CP2_R_P-1;
- a speed measurement is also possible thanks to a micro-turbine flow meter which is installed in the lower part. This measurement technique allows detecting the resultant velocity of the fluid, which flows along its axis. If the fluid hits the micro-turbine in a diagonal direction, it measures a lower velocity.

2.3. Experimental procedure

The containment, the steam generator and the connecting line are initially at ambient temperature and pressure and the valves are closed. The connection line is heated to set a fixed temperature. The steam generator is filled with nitrogen for N_2 experiments until the defined pressure is reached and it is thermalized. The connection line is then pressurized by opening the isolation valve. Once the temperatures and pressures are stabilized, the fast valve, separating the connection line from the containment, is open. The nitrogen contained in the steam generator is injected into the containment. After a delay defined by the experimenters, the fast valve is closed again, stopping the injection of gas. The test continues for some minutes/hours until the containment reaches again the room conditions.

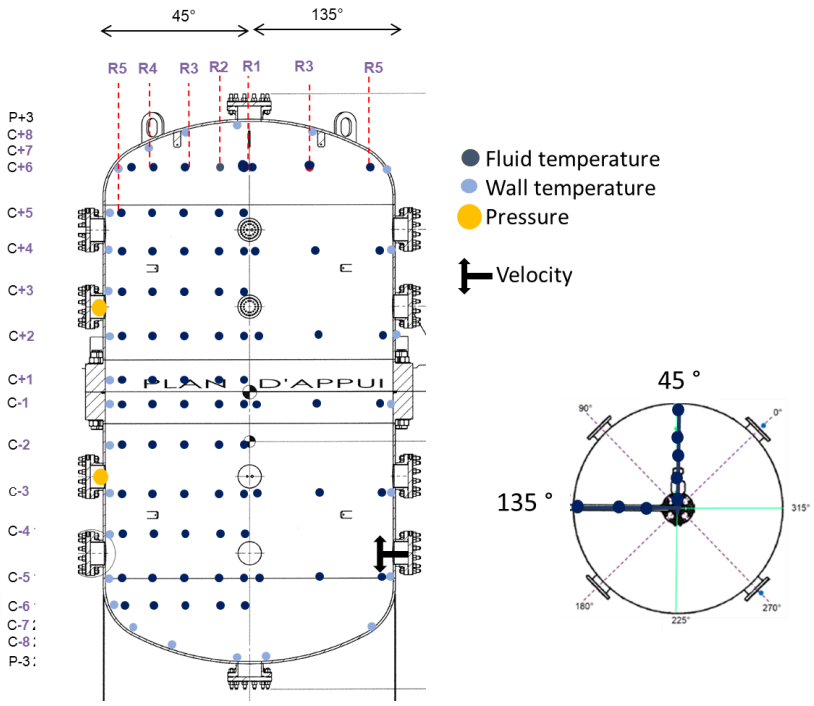

Figure 4: Sketch of RIVA instrumentation for the connection line

3. EXPERIMENTAL ANALYSIS OF A FAST BLOWDOWN WITH NITROGEN

As a started point, nitrogen blowdown experiments are realized. Further experiments with a steam blowdown have been performed to take into account the wall condensation and will be the subject of a future article.

The first series of experiments with nitrogen allows us to characterize the fluid flow through the measurements of pressure, gas temperature and velocity near the containment wall avoiding the effect of steam condensation at the wall. Moreover, measurements can be controlled and compared with analytical solutions.

In this section, two experiences will be described. They differ only for the injection system but initial pressure and temperature are the same. Finally, Test 1 has no particular injection system, thus the connection pipe goes down the containment. In Test 2, the connection line ends with the "jet breaker" described in Section 2.

In the plots below:

- the p^* is the instantaneous pressure scaled with respect to the maximum pressure measured during the Test 1;
- the m^* is the instantaneous mass flow rate scaled with respect to the maximum mass flow rate measured during the Test 1;
- the θ^* is the instantaneous temperature scaled with respect to the room temperature measured during the Test 1;
- the T^* is the instantaneous temperature scaled with respect to the maximum temperature measured during the Test 1;
- the velocity v^* is scaled with respect to the maximum velocity of the Test 1.

3.1. Pressure in the steam generator and in the connection line

Figure 5 represents the evolution of the non-dimensional pressure in different points of the facility. After reaching a stabilized initial pressure in the connection line and in the steam generator, the valve opens (time is set equal to 0s). The CP5_T_P+1 sensor is located just above the fast valve. Therefore, this sensor (green curve) is the first signal to show a change in slope when the transient begins. The others sensors measure quite similar pressure values. The slight differences are due to the pressure drop in the connection line. After roughly 12s, the valve is closed. In Test 2, the evolution of the pressure is the same, since the geometry at end of the connection line does not affect the evolution of the upstream pressure.

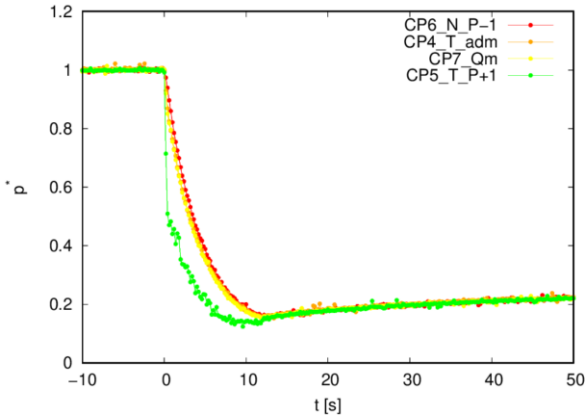

Figure 5: Ratio of pressure and its maximum as a function of time in the steam generator and in connection line for Test 1.

3.2. Comparison of the measured mass flow rate with the analytical solution for the chocked flow

The control of the mass flow rate flowing down in the containment is crucial, since it influences the flow regime and the pressure during the transient. Thanks to the single-phase gas discharge experiments, it is possible to know the downstream/upstream pressure ratio of a section necessary to establish a sonic flow at the outlet with the mass and momentum balance (Hugoniot relation):

$$\frac{P_{downstream}}{P_{upstream}} \leq \left(\frac{2}{\gamma+1}\right)^{\frac{\gamma}{\gamma-1}} \quad (1)$$

in which γ is 1.4 for a diatomic perfect gas.
If Equation 1 holds, the fluid velocity at the sonic section is equal to the sonic velocity: the flow rate no longer depends on the outlet pressure but only on the inlet one. Thus, it exists a value for the pressure ratio (0.528 for a diatomic perfect gas) which separates the sonic flow from the non-sonic flow. Defined the flow area, a sonic flow is installed if the pressure ratio is under 0.528.
The pressure ratio can be calculated at almost all flow restrictions to verify the position of the sonic section (Figure 6): steam generator/connection line inlet, connection line inlet/outlet (to check that no sonic flow settles in the elbows or flow meter), connection line outlet/containment inlet. The sonic flow is presented at the beginning of the discharge at the inlet of the containment, as expected (Figure 6 black line). The sonic period lasts roughly 5s, then the injection continues with a subsonic-jet.

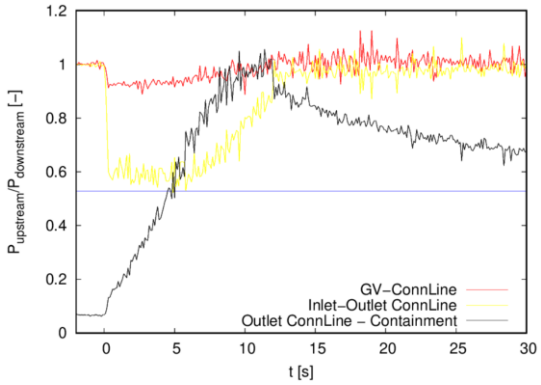

Figure 6: Pressure ratio as a function of time for every section of the connection line.

During the sonic period of the injection, it is possible to determine the flow rate analytically:

$$Q_{crit} = \rho_{upstream} A_{flow} \sqrt{\frac{P_{upstream}}{\rho_{upstream}} \frac{2\gamma}{\gamma-1}\left(1 - \left(\frac{P_{downstream}}{P_{upstream}}\right)^{\frac{\gamma-1}{\gamma}}\right)} \quad (2)$$

In Figure 7, the measurements and the analytical solution agree perfectly, which confirms that the measurements are reliable. Nevertheless, this method is very sensitive to the timing of the experimental signals. It can be noted that when the valve is open, the analytical solution has a delay of about 300ms with respect to the flowmeter. This difference is due to the pressure signals used in Equation 1.
The "jet-breaker" does not affect the mass flow rate and Test 1 and Test 2 are in perfect agreement.

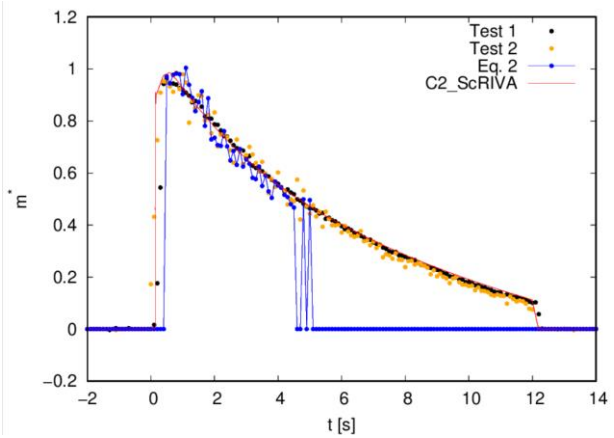

Figure 7: Mass flow rate ratio as a function of time for Test 1 and 2 compared to the Equation 2 and the simulation with CATHARE2.

3.3. Pressure in the containment

The time-evolution of the non-dimensional pressure (Figure 8) initially increases and reaches a maximum before the closure of the fast valve. The slope of pressure changes at about 5s, which corresponds to the moment of transition between a sonic and a subsonic regime at the inlet of the containment (Figure 6). During the period of the sonic injection, the injection velocity drives the containment pressure. On the contrary, during the subsonic period, the pressure of the containment is increased enough to contrast to the injection and the increase slows down.

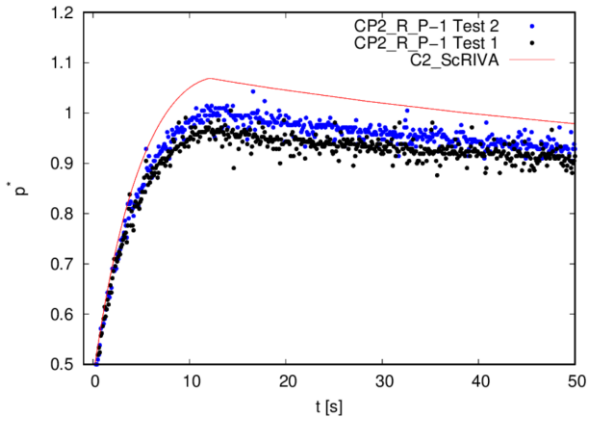

Figure 8: Time-evolution of the pressure in the containment for Test 1 and 2 and the simulation with CATHARE2.

The "jet-breaker" is designed to slow down the jet in the containment, even if the velocity at the outlet of the connection pipe is the same that Test1. With a lower velocity in the containment, a higher pressure is expected. In Figure 8, the comparison between the evolution of the pressure for the test without and with the "jet-breaker" shows a very slight increase in the maximum achieved. The evolution is almost identical in both cases until 5 seconds, before the flow changes from sonic to subsonic one. Then, energy dissipation is higher in the Test 1 than in the Test 2 because the jet velocity is higher. For that reason, Test 2 presents a higher pressure.

3.4. Gas temperature in the containment

The axial temperature profiles in the containment on the 45° axis (Figure 4) at each radius for the Test 1 are shown in Figure 9. Before the N_2 discharge, the containment atmosphere is at room temperature. Once the fast valve opens, it becomes strongly stratified along the injection axis (i.e. R1 red line). During the injection period (about 12 s), the hottest point is the first thermocouple just below the injection at R1. Thermocouples at R2 to R4 have different trends w.r.t. R1 but quite similar trends among themselves (Figure 9): in the upper part (from C+6 to C-1) are colder than in the lower part (from C-2 to C-6). The jet seems to bounce off the lower part of the containment and to wind up the walls without reaching the upper part. The containment seems to be divided into two volumes: an upper part with a recirculation between the cold wall and the hot jet and a more homogeneous lower part directly linked to the jet speed before 19s. Thermocouples at the most external radius (R5) are the coldest in the lower part due to the wall heat exchange. On the contrary, in upper part, the fluid heats up next to the wall due to the recirculation zone. Once the valve is closed (see plots at 19s and later), the flow tends to stratify vertically and is driven by the heat exchange at the wall. Natural circulation is installed in the whole containment, with recirculation vortex between R1 and R5.

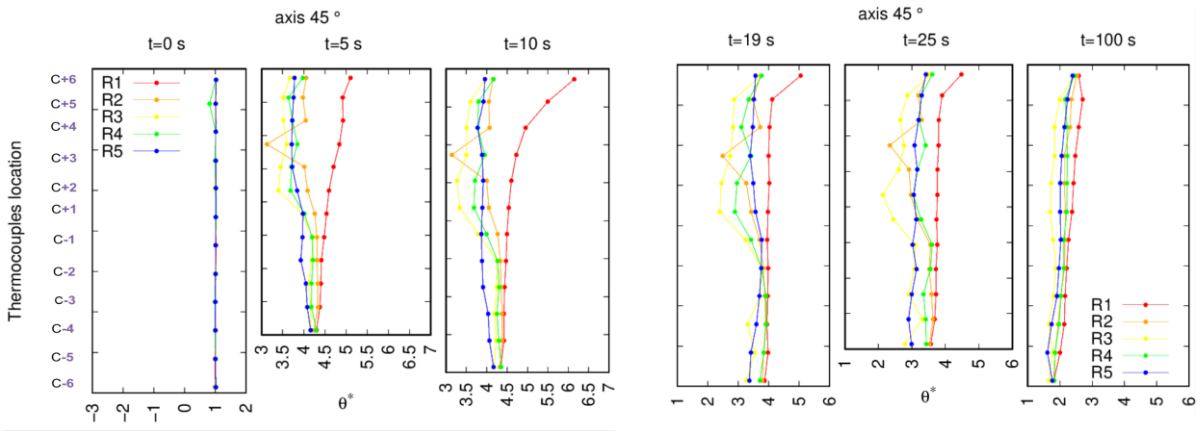

Figure 9: Axial temperature profiles of the gas in the containment for Test 1 at different time. X-axis has the same scale except at t=0s

The time-evolution of the temperature along the injection axis is presented in Figure 10. The hottest temperature is the one nearest the injection pipe (red line). At the two highest measurement points along the injection axis (M+6_R1 and M+5_R1), the temperature decreases due to the sonic jet decompression of the atmosphere. At M+4_R1, this phenomenon is quite faded. Once the chocked flow finishes, the temperature at M+6_R1 continues to increase until the end of the discharge. The other temperatures along the radius R1 (from M+3 to M-6) show a slower increase of the temperature and they reach a maximum during the sonic period.

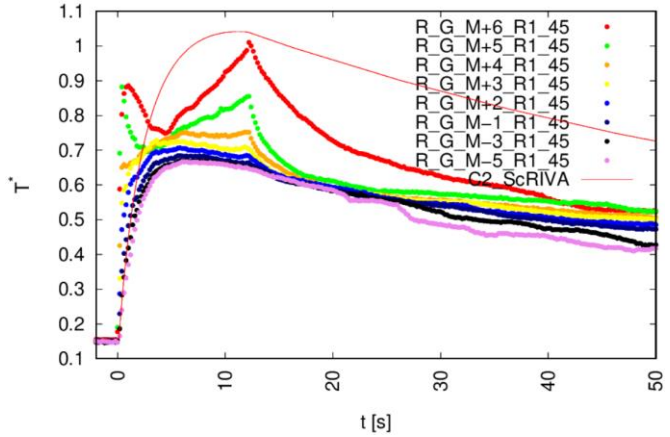

Figure 10: Time-evolution of the temperature along the symmetrical axis at 45° angle of the containment for Test 1 compared to the simulation with CATHARE2.

For Test 2 with the "jet-breaker", the development of fluid flow in the containment is different. During the sonic period (Figure 11 until 5s), the sonic jet hits the walls in the upper part of the containment with a quite horizontal direction. Indeed, at 5s the thermocouples near the wall (R5) are the hottest one. Nevertheless, as the jet does not reach the bottom of the containment, a recirculation zone takes place in the upper part. This recirculation is directly linked to the jet speed and to its dynamics. The lower part stratifies vertically. When the jet is no longer sonic (after 5s in Figure 11), it seems that the injection is no longer directed towards the caps, but that part of the jet goes towards the bottom. This phenomenon is observed for low flow rates and would explain the fact that at 10 s the thermocouples located on the R1 radius are hotter than ones at R5. After the valve is closed, the wall exchange drives the flow and the containment stratifies horizontally and vertically.

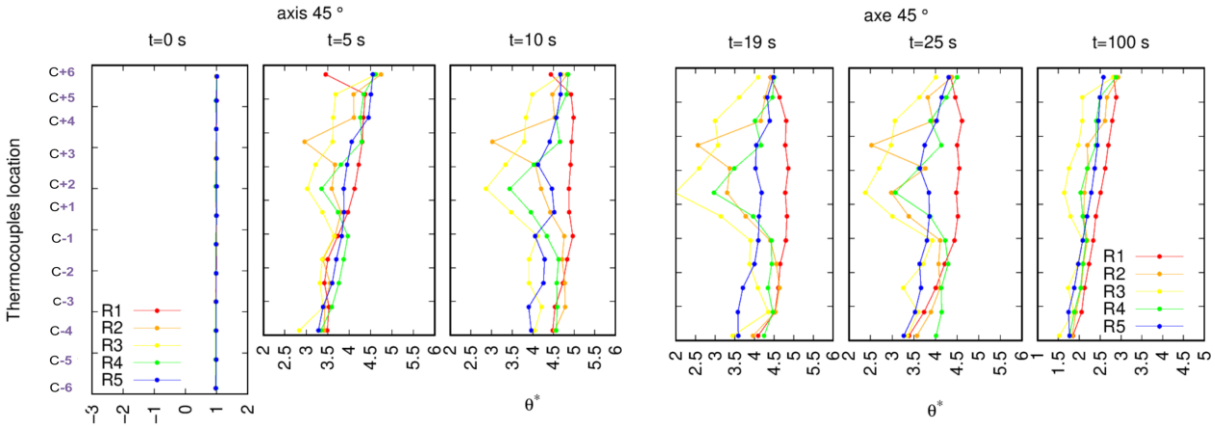

Figure 11: Axial temperature profiles of the gas in the containment for Test 2 at different time. X-axis has the same scale except at t=0s

The time-evolution of the temperature along the most external radius of the gas atmosphere of the containment is shown in Figure 12. At the beginning of the injection, the thermocouples heat up when the fluid flows down along the wall. For that reason, during the sonic period, the hottest thermocouples are the highest one. Then, the jet reaches the lower part of the containment, but not the lowest one. Thus, the lower part of the containment is colder than the higher one, even near the wall.

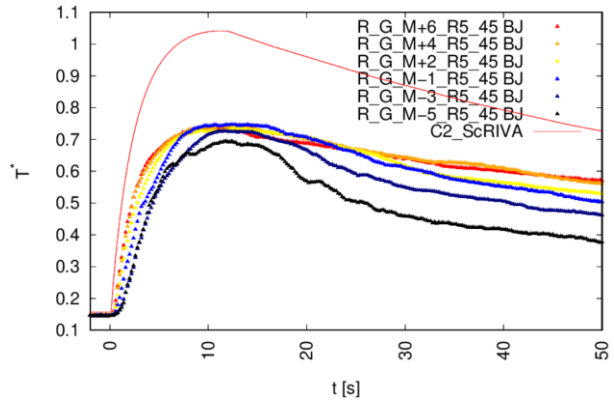

Figure 12: Time-evolution of the temperature along the most external (R5) radius at axis at 45° angle of the containment for Test 1 compared to the simulation with CATHARE2.

3.5. Measurement of velocity near the wall of the containment

The near-wall velocity measurement (30 mm from the wall of the containment) at the lowest position available (i.e. P-2) provides a better understanding of the flow dynamics for the two tests. It is important to note that the micro-turbine flow meter can measure only the resultant velocity of the fluid, as explained in Section 2.2.

During the Test 1 (Figure 13a), the maximum velocity is obtained at roughly 5s, i.e. at the end of the sonic period. Then, the nitrogen slows down. After some seconds, the velocity rises up. It can be explained by the change in the direction of the velocity. The second peak may occur because the natural convection has begun. After the valve closes (at 12s), the velocity decreases. A change in slope is visible when the valve is closed. At 18s, the wall velocity is zero.

For the Test 2 (Figure 13b), the wall velocity is zero during the entire experiment. It confirms that the jet does not reach the bottom of the containment.

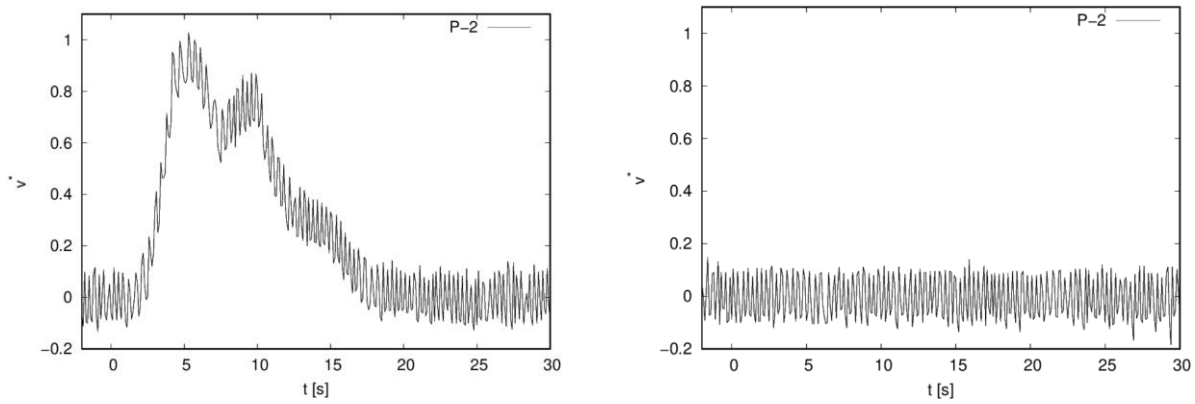

a) Test 1 b) Test 2

Figure 13: Velocity profiles of the fluid at the bottom of the containment near the wall for Test 1 and 2.

4. COMPARISON BETWEEN EXPERIMENTS AND THE SYSTEM CODE CATHARE2

The RIVA experiments are compared with the system code CATHARE2 [4] used for the safety studies of the French nuclear fleet. In particular, the comparison focuses on the pressure and the temperature peaks in order to verify the consistency and the possible improvement of the modelling and the code. In this section, the description of the computer model and the results of the simulations are discussed.

4.1. Description of the RIVA modelling with CATHARE2

The system code CATHARE2 [15] solves the 6-equations model (mass, momentum and energy balance for two fluid components). It allows reproducing a nuclear reactor in normal and accidental conditions. It models complex phenomena in two-phase flow, such as the critical flow, the reflooding in the core, etc… It is also used for the physical analysis of the several accidents, in particular for simulating the behavior of the fluid flow in the containment [4].
To simulate the discharge of nitrogen in the RIVA facility with CATHARE2, the nodalization is modelled by:

- an axial 1D steam generator with variable flow section;
- several axial 1D components composing the connection line;
- a 0D volume representing the containment. The volume and the heat exchange area are equivalent to experiments to avoid distortions.

The local pressure drop are calibrated with [16] to reproduce the trend of the pressure in the line.
The injection system is not specifically simulated. Therefore, the input date is the same for the Test 1 and Test 2. However, the distribution of the flow near the wall containment is taken into account through the definition of the velocity in the correlation of the wall heat exchange.
The simulation starts by filling the steam generator with nitrogen at the target pressure and bringing the connection line to temperature, as in the experience. A non-flow boundary condition is then set on the steam generator to isolate it from the rest of the CIRCUIT (Figure 15). The receiver is initialized. Then the boundary condition is changed to BLIND and the containment is isolated. From this point on, the transient begins.
During roughly 200s, which is the time in the experiment between the opening of the isolation valve and the fast valve, a stabilized transient is calculated. After, the fast valve opens almost instantaneously and gas is injected into the containment.

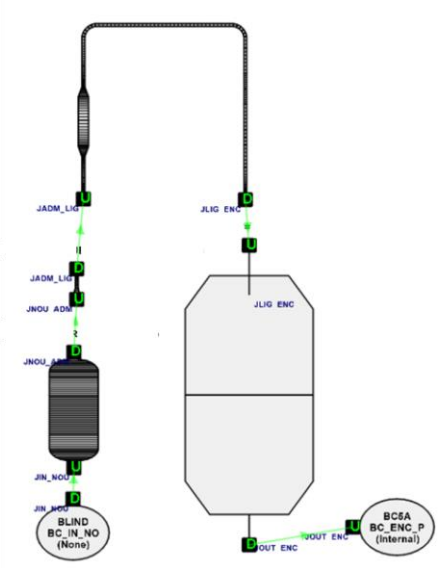

Figure 14: Sketch of the RIVA modelling with CATHARE2.

4.2. Comparison of RIVA experience with CATHARE2

The comparison between the experiment and the simulation in CATHARE2 (Figure 15) shows a slight overestimation of the pressure of the steam generator. Nevertheless, the agreement between the two curves is acceptable.

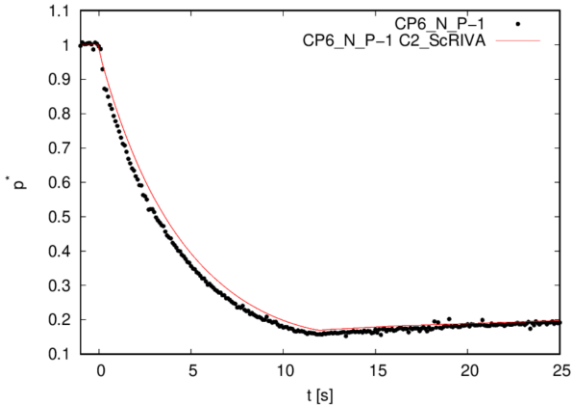

Figure 15: Comparison between the experimental and simulated time evolution of the steam generator pressure

A good agreement is shown in Figure 7 between the simulation and experiments for the mass flow rate. Since the discharge pressure is slightly higher in the simulation, the containment pressure is expected to be higher in order to simulate the right experimental mass flow rate. Actually, Figure 8 shows a higher pressure in the simulation than in the experiments. Nevertheless, evolutions are in very good agreement, especially during the first seconds of the discharge. During this period, the heat exchange at the wall is not efficient and the containment pressurizes in a quite adiabatic condition. When the heat exchange becomes efficient, the pressure increase is reduced but not in CATHARE2. This phenomenon is shown also in Figure 10 and Figure 12 with the comparison of the temperatures. CATHARE2 simulates only one temperature for the gas, giving an average estimation of the whole temperatures in the containment. The overestimated pressure results in an overestimated gas temperature in the containment for Test 1 and Test 2 after the efficient period

of the heat exchange. To improve the results with CATHARE2 code, works on correlations of heat exchange at the wall will be performed.

5. CONCLUSION

In case of Main Steam Line Break scenarios, several thermal hydraulics phenomena are extensively studied for large containment safety analysis. Nevertheless, there is a lack of experimental data and analysis for compact reactors. In this framework, the RIVA facility is built to investigate the fast blowdown of a steam generator discharging in a small containment. The facility is highly instrumented. An instrumentation section on the connection pipe allows us to measure local pressure, pressure drop and local temperature before the inlet of the vessel. Different injection system are available to analyze the effect of the direction of the jet.

As a started point, nitrogen blowdown experiments are realized. The chocked flow is installed at the inlet of the containment. During the sonic injection, pressure and temperature increase in the containment. For the Test 1 (injection with pipe), the jet hits the lowest wall, bounces off and winds up until the middle height. The nitrogen jet drives the pressurization and the heat exchange at the wall via the recirculation zone. For Test 2, the jet flows down but not completely in the lower part. The heat exchange at the wall is driven by jet, which flow downs over the wall. Simulations are performed with CATHARE2, simulating the containment with a 0D volume. A good agreement for pressure and temperature is found, even if improvement in correlations for heat exchange can be done.

Yet, the final goal is to perform fast one-phase steam blowdown and fast pressurization of the containment, as in [14]. Additional experimental tests have been performed to improve the knowledge of small containment behavior and will be present in future papers.

DATA AVAILABILITY

The data that support the findings of this study are available from the corresponding author upon reasonable request.

REFERENCES

[1] "Defence in Depth in Nuclear Safety INSAG-10 A report by the International Nuclear Safety Advisory Group." IAEA, 1997. [Online]. Available: https://www-pub.iaea.org/mtcd/publications/pdf/pub1013e_web.pdf

[2] Y.-C. Park, D.-S. Song, and H.-Y. Jun, "Main Steam Line Break Mass/Energy and Pressure/Temperature Analysis for the Environmental Qualification," in *Transactions of the Korean Nuclear Society Spring Meeting*, Chuncheon, Korea, May 2006.

[3] D. Papini, M. Andreani, B. Niceno, and H. M. Prasser, "Evaluation of the Hydrogen Risk in Containment for Small Break LOCA Sequences Using the GOTHIC Code," in *NURETH-17*, 2017, pp. 3–8.

[4] U. Bieder and F. Barre, "Adaptation of CATHARE 2 to the containment Qualification of the models," presented at the NURETH-8, Japan, Japan: Atomic Energy Society of Japan, 1997.

[5] M. Andreani, A. Badillo, and R. Kapulla, "Synthesis of the OECD/NEA-PSI CFD benchmark exercise," *Nucl. Eng. Des.*, vol. 299, pp. 59–80, Apr. 2016, doi: 10.1016/j.nucengdes.2015.12.029.

[6] S. Abe, E. Studer, M. Ishigaki, Y. Sibamoto, and T. Yonomoto, "Stratification breakup by a diffuse buoyant jet: The MISTRA HM1-1 and 1-1bis experiments and their CFD analysis," *Nucl. Eng. Des.*, vol. 331, pp. 162–175, May 2018, doi: 10.1016/j.nucengdes.2018.01.050.

[7] S. Kudriakov *et al.*, "The TONUS CFD code for hydrogen risk analysis: Physical models, numerical schemes and validation matrix," *Nucl. Eng. Des.*, vol. 238, no. 3, pp. 551–565, Mar. 2008, doi: 10.1016/j.nucengdes.2007.02.048.

[8] E. Studer *et al.*, “Challenges in Containment Thermal Hydraulics,” *Nucl. Technol.*, vol. 206, no. 9, pp. 1361–1373, Sep. 2020, doi: 10.1080/00295450.2020.1731406.
[9] J. Malet, E. Porcheron, and J. Vendel, “OECD International Standard Problem ISP-47 on containment thermal-hydraulics—Conclusions of the TOSQAN part,” *Nucl. Eng. Des.*, vol. 240, no. 10, pp. 3209–3220, Oct. 2010, doi: 10.1016/j.nucengdes.2010.05.061.
[10] D. Paladino, R. Kapulla, S. Paranjape, S. Suter, and M. Andreani, “PANDA experiments within the OECD/NEA HYMERES-2 project on containment hydrogen distribution, thermal radiation and suppression pool phenomena,” *Nucl. Eng. Des.*, vol. 392, p. 111777, Jun. 2022, doi: 10.1016/j.nucengdes.2022.111777.
[11] T. Kanzleiter *et al.*, *OECD/NEA THAI Project Hydrogen and Fission Product Issues Relevant for Containment Safety Assessment Under Severe Accident Conditions*. OECD, Boulogne-Billancourt, France, 2010.
[12] B.-U. Bae, J. B. Lee, Y.-S. Park, J. Kim, and K.-H. Kang, “Integral effect test for steam line break with coupling reactor coolant system and containment using ATLAS-CUBE facility,” *Nucl. Eng. Technol.*, vol. 53, no. 8, pp. 2477–2487, août 2021, doi: 10.1016/j.net.2021.02.020.
[13] Y. Fang *et al.*, “Experimental study of heat transfer in the complex space of small steel containment with a steam jet,” *Ann. Nucl. Energy*, vol. 166, p. 108822, février 2022, doi: 10.1016/j.anucene.2021.108822.
[14] M. Zhu, H. Chang, H. Wang, Q. Zhu, and J. Wang, “Steam condensation separate effect tests in core make-up tank,” *Prog. Nucl. Energy*, vol. 142, p. 104031, décembre 2021, doi: 10.1016/j.pnucene.2021.104031.
[15] G. Geffraye *et al.*, “CATHARE 2 V2.5_2: A single version for various applications | Elsevier Enhanced Reader,” vol. 241, no. 11, pp. 4456–4463.
[16] I. E. Idel’cik, *Memento des pertes de charge*, Eyrolles. in Collection de la direction des études et recherches d’électricité de France. 1969.